Cell Communication and Signaling

RESEARCH

Open Access

NLRP3, conveyed via extracellular vesicles from metabolic syndrome patients, is involved in atherosclerosis development

Xavier Vidal-Gómez[1,2], Luisa Vergori[2], Séverine Dubois[3], Frédéric Gagnadoux[2,3], Samir Henni[3], Reuben Veerapen[4], Olivier Meilhac[5], Mercedes Muñoz-Picos[2], Concepción Peiró[6], M. Carmen Martinez[1,2], Ramaroson Andriantsitohaina[1,2*] and on behalf of Metabol Study Group

Abstract

Background Inappropriate activation of the Nod-like receptor protein 3 (NLRP3)-inflammasome contributes to atherosclerosis progression and plaque instability in patients with cardiovascular events. However, its role in the atherosclerosis is not fully understood. We sought to uncover actionable targets that could help to refine the diagnostic values of metabolic syndrome (MetS) patients by taking advantage of extracellular vesicles (EVs) to support the inflammatory hypothesis of atherosclerosis.

Methods Circulating large (lEVs) and small (sEVs) EVs from non-MetS subjects and MetS patients were isolated and characterized. The involvement of NLRP3 in the effects of EVs on human aortic endothelial and smooth muscle cells (SMC) and macrophages were analyzed. The pathological relevance in human atherosclerotic lesions was investigated.

Results Circulating levels of lEVs carrying NLRP3 correlated with metabolic risk factors associated with obesity and insulin resistance. Both types of EVs from MetS patients increased endothelial permeability, monocyte transmigration, SMC migration and secretion of pro-inflammatory molecules by monocyte/macrophages. Interestingly, MetS-lEVs, but not MetS-sEVs, increased SMC proliferation and IL-1ß production. EVs isolated from advanced human plaques demonstrated an accumulation of EVs carrying NLRP3 and their implication in endothelial permeability increase. Pharmacological inhibition of NLRP3-inflammasome carried by MetS-EVs prevented all the effects leading to vascular inflammation and remodeling.

Conclusions Our data demonstrate that NLRP3-inflammasome, carried by EVs, is actively involved in vascular inflammation and atherosclerosis development in MetS. We highlight NLRP3 carried by EVs as potential biomarker and target for potential therapeutic strategies of atherosclerosis-related diseases leading to major adverse cardiovascular events.

Keywords NLRP3, Extracellular vesicles, Metabolic syndrome, Vascular inflammation, Atherosclerosis development

*Correspondence:
Ramaroson Andriantsitohaina
ramaroson.andriantsitohaina@inserm.fr

Full list of author information is available at the end of the article

Graphical Abstract

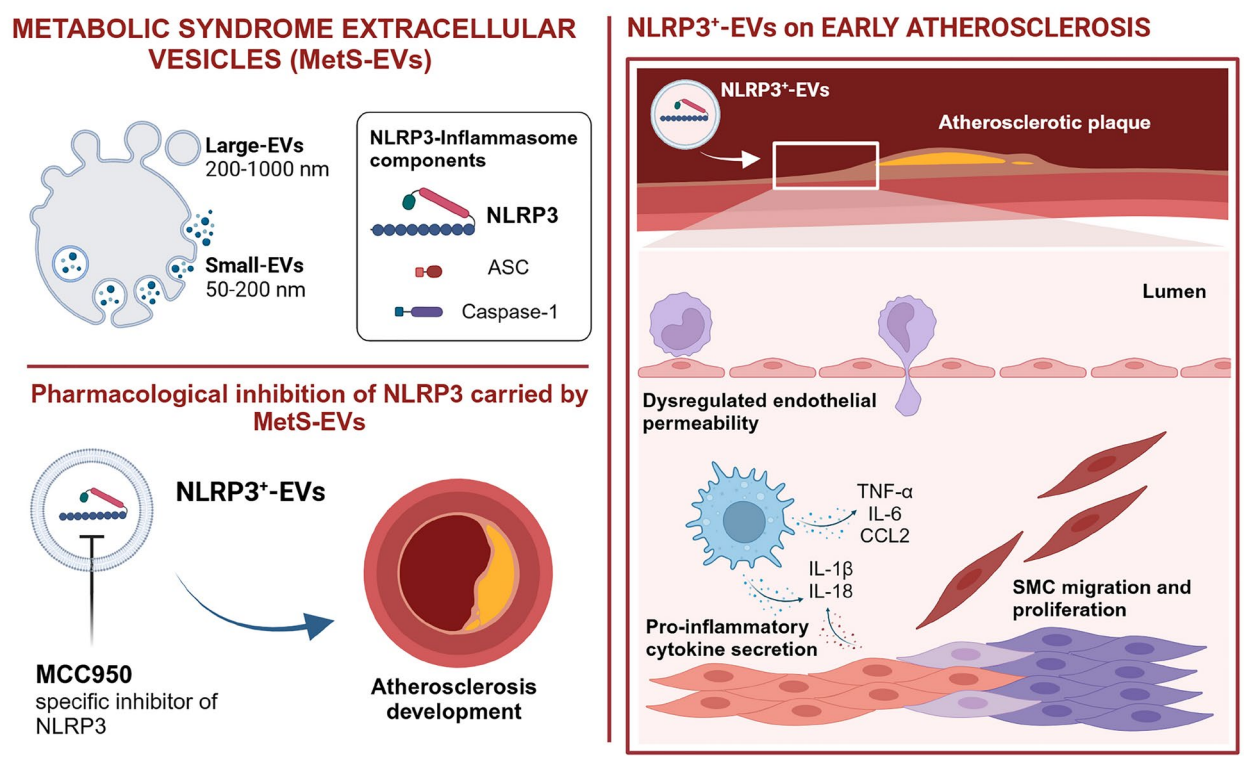

Introduction

Obesity increases the risk of metabolic dysregulation, including insulin resistance, hypertriglyceridemia, and low plasma high-density lipoprotein cholesterol (HDL-c) concentrations. These metabolic abnormalities, collectively referred to as the metabolic syndrome (MetS) and are associated with an increased risk of developing atherosclerotic cardiovascular diseases (CVD) [1, 2]. Current pharmaceutical interventions designed to slowdown the progression of atherosclerosis focus almost exclusively on lowering plasma cholesterol levels [3].

Three recent randomized, double-blind, controlled clinical trials, the Canakinumab Anti-inflammatory Thrombosis Outcomes Study (CANTOS), the Cardiovascular Inflammation Reduction Trial (CIRT), and the Colchicine Cardiovascular Outcomes Trial (COLCOT), show that the anti-inflammatory therapy may be an effective therapeutic strategy for secondary prevention at high-risk patients for cardiovascular events [4–6]. While not pure inflammasome inhibitors, the parenterally administered canakinumab, rilonacept, and anakinra deserve honorable mention as blockers of IL-1ß because this inflammatory cytokine is a product of NLRP3 inflammasome activation. As reviewed by Dri et al. [7], the molecule colchicine disrupts tubulin, thereby reducing the migration and replication of inflammatory cells. This action, among others that are not yet well defined, affects endothelial function and inhibits the NLRP3 inflammasome [8]. Another effect is an indirect reduction in the activation of IL-1ß and downstream in IL-6 and CRP, known mediators that activate macrophages and propagate atherosclerosis. Final data from clinical trials with MCC950 and other NLRP3 inflammasome inhibitors such as IFM-2427, RRX-001, Inzomelid, Dapansutrile® and Somalix have not yet been reported. Thus, the inflammasome pathway is a promising target for further anti-inflammatory interventions to reduce atherothrombosis. Indeed, inappropriate activation of the NLRP3-inflammasome can contribute to the onset and progression of various diseases, particularly age- and metabolic-related diseases such as MetS [9]. Although Menu et al. were the first to describe the progression of atherosclerosis in apolipoprotein E-deficient mice as being independent of the NLRP3 inflammasome [10], Zheng et al. later reported that the suppression of the NLRP3 inflammasome led to the suppression of atherosclerosis and the stabilization of plaques in apolipoprotein E-deficient mice [11]. Furthermore, increased production of IL-1β and IL-18 following NLRP3-inflammasome activation has been shown to contribute to atheroma formation, arteriosclerosis progression, and plaque instability in atherosclerotic patients and animal

models [12, 13]. These data support the hypothesis of a potential link between the NLRP3-inflammasome and atherosclerosis development. Extracellular vesicles (EVs), including large (lEVs) and small (sEVs), are membrane-bound vesicles released by most cell types and have been described as critical players in the early stages of atherosclerotic development and progression [14, 15]. We have described that circulating lEVs and sEVs levels are increased in MetS patients, especially pro-coagulant and pro-inflammatory EVs [16, 17]. We have reported that circulating lEVs from MetS patients (MetS-lEVs) carrying Fas ligand induce endothelial dysfunction by interacting with the Fas receptor on endothelial cells, leading to a temporal crosstalk between the endoplasmic reticulum and mitochondria via the activation of neutral sphingomyelinase and reducing nitric oxide release [18]. We have also demonstrated that Rap1 carried by MetS-lEVs may be a novel determinant of diagnostic value for cardiometabolic risk factors and a promising therapeutic target against atherosclerosis [19]. For sEVs, we have highlighted that lipopolysaccharide (LPS)-enriched sEVs from MetS patients induce endothelial dysfunction through activation of TLR4 receptor and may be responsible, at least in part, for the low endotoxemia-induced oxidative stress described in these patients [17]. The potential role of NLRP3 carried by lEVs as transducers of inflammatory signals leading cardiovascular risk factors to vascular injury has been reported in vitro. Indeed, LPS has been shown to induce the NLRP3$^+$-lEV release by monocytes and activate endothelial cells [20]. Knockdown of NLRP3 in THP-1 monocytic cells reduces the activity of lEVs and decreases lEV-dependent induction of cell adhesion molecules by blocking the IL-1R on endothelial cells. Silvis et al. [21] reported that colchicine reduced EV-associated NLRP3-inflammasome protein levels in chronic coronary disease. However, these authors have only analyzed CD9$^+$-EVs that represent sEV populations and the relative contribution of lEVs and sEVs carrying NLRP3 remains to be elucidated.

In the present study, we investigated whether the NLRP3-inflammasome carried by MetS-EVs may be responsible, at least in part, for the enhanced vascular remodeling and inflammation described in atherosclerotic patients and for the MetS-associated impairment of endothelial cells, vascular smooth muscle cells (SMC) and monocyte/macrophages function.

Results

As previously described, MetS patients displayed significantly increased visceral obesity (elevated BMI and waist circumference), insulin resistance (elevated glycemia and glycated hemoglobin - HbA1c), and dyslipidemia (elevated triglyceride levels and decreased plasma HDL-cholesterol levels) (Table 1). As expected, lEV size (300–800 nm) was higher than those of sEVs (70–200 nm) (Supplemental Fig. 1A to C). In addition, size of both types of EVs from MetS was lower than those of nMetS subjects (Supplemental Fig. 1C to F). Confirming our previous results, lEVs were enriched in the cytoskeletal protein ß-actin and the GTPase Rap1, whereas sEVs had enhanced expression of sEV specific markers such as TSG101, CD63, CD9 and CD81 (Supplemental Fig. 1G and H). Circulating levels of MetS-lEVs and MetS-sEVs were significantly higher compared to nMetS subjects (Table 1). MetS patients showed an increased proportion of lymphocyte-, monocyte-, granulocyte-, platelet-, endothelial- and erythrocyte-derived lEVs compared to nMetS donors (Supplemental Fig. 1I). Non-statistical differences were found in other specific cell markers analyzed in circulating lEVs, such α-smooth muscle actin (Supplemental Fig. 1I) or the pro-coagulant phosphatidylserine (Annexin-V$^+$) (Supplemental Fig. 1J).

NLRP3-inflammasome components are differently expressed between lEVs and sEVs

Circulating MetS-lEV levels expressing NLRP3 were significantly higher than those from nMetS subjects (Fig. 1A). Permeabilization of lEVs with saponin showed that NLRP3 was essentially carried inside the vesicles (Supplemental Fig. 2). In MetS patients, levels of lymphocyte (CD4$^+$)-, monocyte (CD14$^+$)-, and activated endothelial cell (CD144$^+$)-derived lEVs carrying NLRP3 were increased when compared to nMetS individuals (Fig. 1B). This increase in circulating NLRP3$^+$-lEVs correlated with the number of MetS criteria (Fig. 1C) and was confirmed by Western blot (Fig. 1D and E). Interestingly, both EV types from nMetS and MetS patients expressed, all components of NLRP3-inflammasome including NLRP3, ASC, pro-Caspase-1, Caspase-1, and pro-IL-1ß (Fig. 1D-G). However, MetS-lEVs showed increased levels of NLRP3 and Caspase-1, whereas MetS-sEVs showed increased levels of pro-Caspase-1 and Caspase-1 compared to nMetS-sEVs (Fig. 1F and G). These differences in NLRP3-inflammasome components in both EV types support a relevant involvement of EVs in the sterile inflammatory process associated with MetS.

Circulating NLRP3$^+$-lEV levels correlate with metabolic disorders and cardiovascular risk

Circulating NLRP3$^+$-lEVs were positively correlated with waist and hip circumference, BMI, diastolic blood pressure, glycemia, insulinemia, homeostasis model assessment (HOMA), HbA1c, plasma triglyceride concentration, triglyceride-glucose index (TyG index), and triglyceride/HDL-cholesterol ratio (T/HDL-c ratio), and negatively correlated with plasma HDL-cholesterol concentration (Fig. 2 A-L). Other parameters such as total-cholesterol and LDL-cholesterol did not correlate with

Table 1 Baseline characteristics of non-metabolic syndrome (nMetS) subjects and metabolic syndrome (MetS) patients

	nMetS	MetS	*p*-value
Criteria			
Number	23	26	
Sex ratio (female/male)	6/17	8/18	
Age (years)	59 [52, 64]	53 [44, 64]	0.2066
BMI (kg/m^2)	25.9 [24.5, 29.2]	32.5 [29.2, 34.2]	< 0.0001
Waist circunference (cm)	94 [88, 97]	107 [102, 115]	< 0.0001
Systolic blood pressure (mmHg)	125 [117, 140]	130 [125, 133]	0.5809
Diastolic blood pressure (mmHg)	81 [75, 84]	80 [76, 89]	0.6368
Insulinemia (mU/L)	6.65 [5.21, 9.91]	19.22 [5.89, 79.61]	0.0727
Glycemia (g/L)	0.94 [0.88, 0.99]	1.18 [1.08, 1.30]	< 0.0001
HbA1c (% of total Hb)	5.6 [5.4, 5.8]	6.1 [5.8, 6.4]	0.0008
Total cholesterol (g/L)	1.91 [1.75, 2.08]	1.75 [1.61, 2.04]	0.3470
HDL-cholesterol (g/L)	0.54 [0.46, 0.58]	0.39 [0.39, 0.43]	< 0.0001
LDL-cholesterol (g/L)	1.16 [0.93, 1.35]	0.93 [0.89, 1.20]	0.1958
Triglycerides (g/L)	1.03 [0.69, 1.25]	1.72 [1.44, 2.20]	< 0.0001
Plasma EV concentration			
lEVs (events/µL plasma) x10^3	21.2 [16.4, 29.1]	32.9 [24.7, 51.4]	0.0337
sEVs (particles/mL plasma) x10^8	9.7 [3.0, 25.4]	31.1 [14.7, 50.4]	0.0012
Number of MetS components (%)			
0	10		
1	14		
2	23		
3		12	
4		29	
5		12	
Treatments (%)			
Oral antidiabetic	13	58	
Antihypertensive	30	54	
Statins	30	38	

Data are expressed as median [IQR] or %. Statistical significance ($p < 0.05$) was tested with unpaired Student's t-test or Mann-Whitney U test as appropriate

total EV levels (Supplemental Table 1) and NLRP3$^+$-lEV levels (Supplemental Table 1). These results indicate that NLRP3$^+$-lEV levels increase with obesity, diastolic blood pressure, insulin resistance, and dyslipidemia, suggesting that they are associated with an increased risk of cardiovascular events.

MetS-EVs increase endothelial cell permeability and monocyte transendothelial migration in a NLRP3-dependent mechanism

The role of circulating NLRP3-EVs on endothelial cell integrity was assessed after stimulation with lEVs and sEVs from nMetS subjects and MetS patients. Both types of MetS-EVs, but not those from nMetS subjects, significantly decreased the transendothelial electrical resistance (TEER) (Fig. 3A). Preincubation with the specific inhibitor of NLRP3, MCC950, of EVs (MCC-EVs) or endothelial cells (MCC-cells), completely prevented the decrease in TEER induced by MetS-lEVs and MetS-sEVs (Fig. 3A). Furthermore, MetS-EVs increased monocyte transmigration across the endothelial cell monolayer (Fig. 3B), and these effects were abolished by the pretreatment of EVs or endothelial cells with MCC950 (Fig. 3B). nMetS-EVs did not affect monocyte transmigration across the endothelial cell monolayer (Supplemental Fig. 3). Notably, MCC950 alone or in the presence of nMetS-EVs did not affect endothelial cell permeability nor monocyte transmigration (Supplemental Fig. 3). These results suggest a mechanism sensitive to MCC950 in the altered endothelial integrity and monocyte transmigration induced by MetS-EVs. Furthermore, these results suggest that MetS-EVs activate the NLRP3-inflammasome pathway on endothelial cells.

NLRP3 carried by MetS-EVs promotes SMC migration and proliferation, and increases pro-inflammatory cytokine production

To evaluate the role of NLRP3$^+$-EVs in vascular remodeling, the effects of EVs from nMetS subjects and MetS patients were assessed on human aortic SMC for migration, proliferation, and inflammatory responses in absence and in the presence of MCC950. The wound healing assay showed that MetS-EVs, but not nMetS-EVs, significantly increased SMC migration like the positive

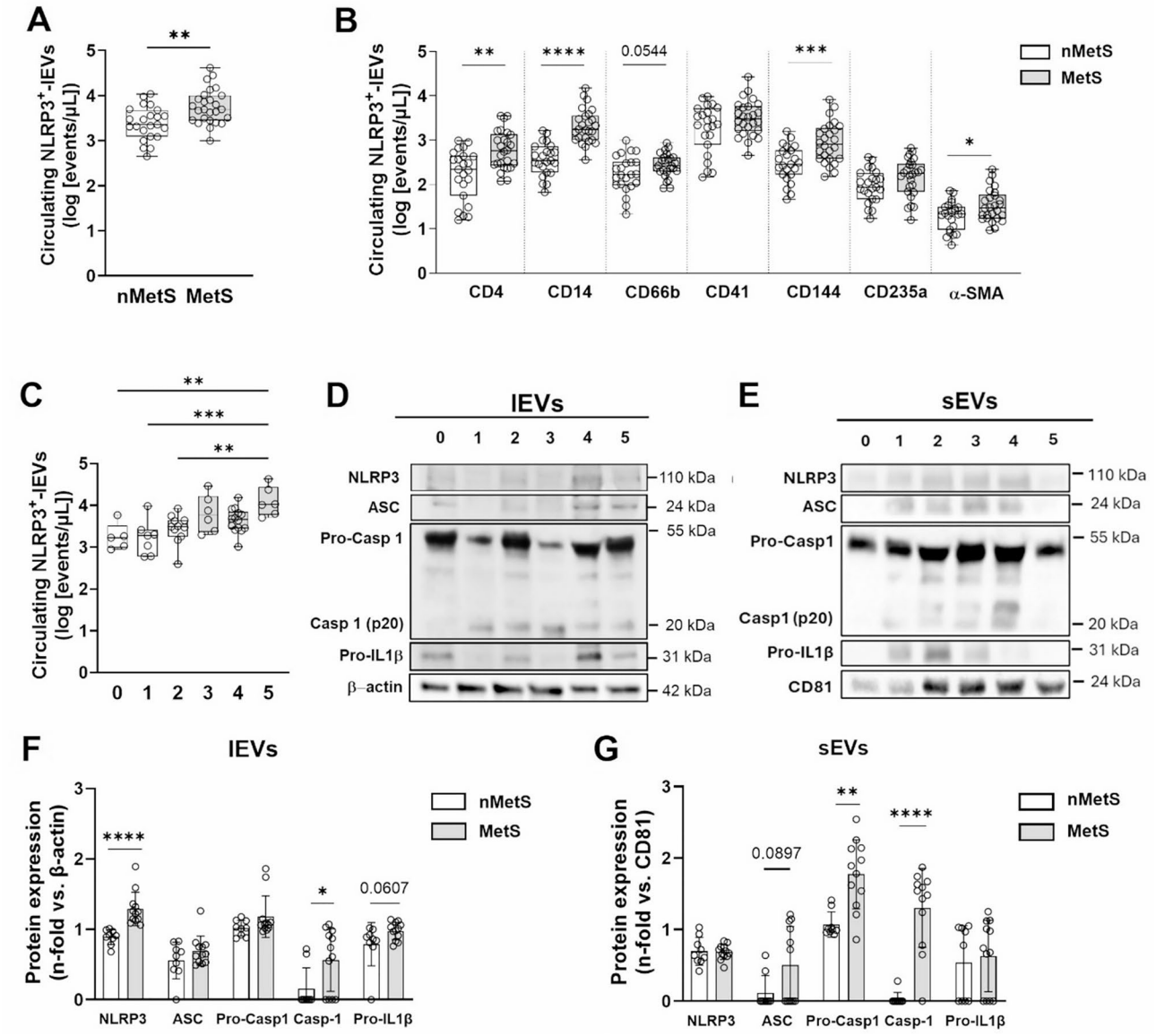

Fig. 1 NLRP3 expression in EVs from metabolic syndrome (MetS) patients. (**A** to **C**) Quantification of (**A**) total and (**B**) cellular origins of circulating large-EVs (lEVs) carrying NLRP3 and (**C**) correlation with the number of components of MetS. NLRP3 levels in lEVs were detected by flow-cytometry. nMetS-lEVs ($n=23$), MetS-lEVs ($n=26$). (**D** and **E**) Representative immunoblot of NLRP3-inflammasome components (NLRP3, ASC, Caspase-1 (p50 and p20) and pro-Interleukin (IL)-1β) expression in (**D**) lEVs and **(E)** small-EVs (sEVs) depending on the number of MetS criteria (0 to 5). β-actin and CD81 were used as housekeeping for lEVs and sEVs, respectively. (**F** and **G**) Histograms showing the quantification of NLRP3-inflammasome components in EVs from nMetS (≤ 2 criteria, $n=9$) and MetS patients (≥ 3 criteria, $n=12$). Data are shown as mean ± SD. Statistical significance was tested with unpaired Student's t-test, Mann-Whitney U test, and 1-way ANOVA followed by Tukey post hoc test as appropriate. *$p<0.05$, **$p<0.01$, ***$p<0.001$ and ****$p<0.0001$

control PDGF-BB (Fig. 4A and B; Supplemental Fig. 4A to F). Pre-incubation of either EVs (MCC-EVs) or SMC with MCC950 (MCC-cells) completely abolished the migration induced by MetS-lEVs without affecting the effects of MetS-sEVs on SMC migration (Fig. 4A and B). Regarding SMC proliferation, only MetS-lEVs significantly increased cell proliferation compared to nMetS-EVs or MetS-sEVs (Fig. 4C). Again, the pre-incubation of either EVs (MCC-EVs) or SMC with MCC950 (MCC-cells) completely prevented the effect of MetS-lEVs (Fig. 4C).

NLRP3-inflammasome activation leads to the release of IL-1ß and IL-18. As control, LPS but not MCC950 significantly enhanced IL-1ß and IL-18 (Supplemental Fig. 5A). The ability of EVs to activate the NLRP3-inflammasome in human aortic SMC was assessed by analyzing the release of these pro-inflammatory cytokines. nMetS-EVs did not induce an elevation of IL-1ß

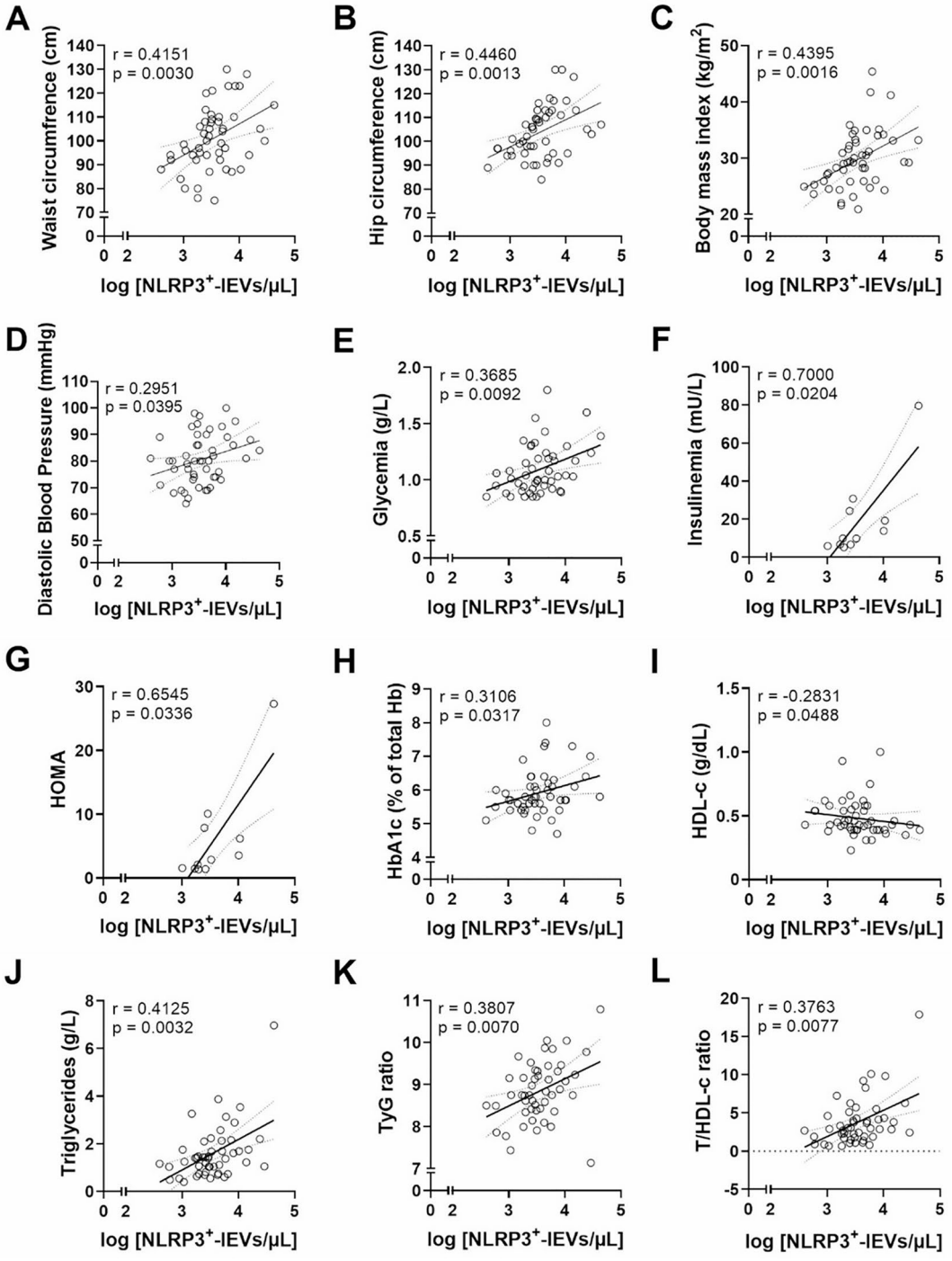

Fig. 2 Correlations between circulating levels of NLRP3^{+}-large extracellular vesicles (lEVs) and clinical parameters. Correlations were performed between levels of NLRP3 and waist circumference (cm) (**A**), hip circumference (cm) (**B**), body mass index (kg/m^{2}) (**C**), diastolic blood pressure (mmHg) (**D**), glycemia (g/L) (**E**), insulinemia (mU/L) (**F**), HOMA index (**G**), glycated hemoglobin (HbA1c, % of total hemoglobin) (**H**), high-density lipoprotein-cholesterol (HDL-c, g/dL) (**I**), plasma triglyceride levels (g/L) (**J**), triglyceride-glucose (TyG) index (**K**) and triglycerides/HDL-cholesterol (T/HDL-c) ratio (**L**). Correlations were performed by Pearson correlation test. ($n = 49$)

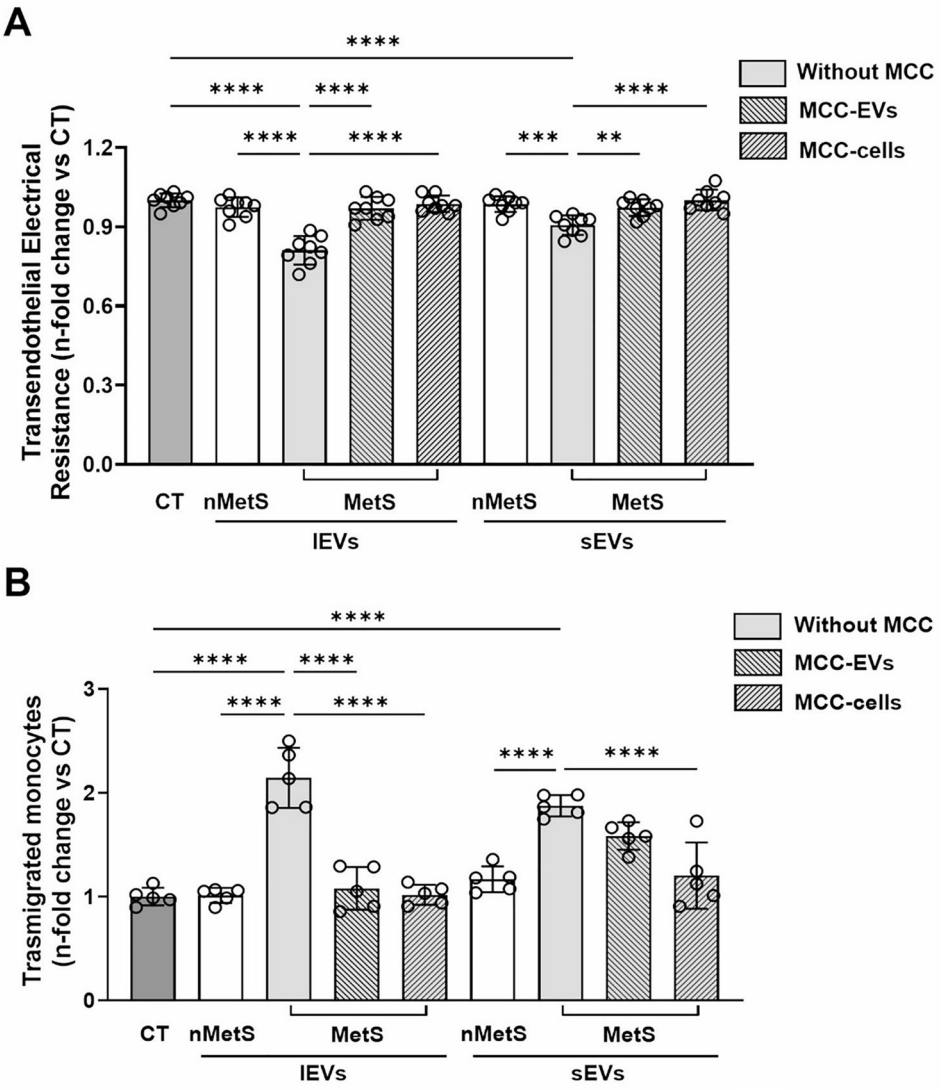

Fig. 3 Effect of NLRP3^{+}-extracellular vesicles (EVs) on endothelial permeability. (**A**) Changes on endothelial permeability measured by transendothelial electrical resistance induced by large-EVs (lEVs) and small-EVs (sEVs) from non-metabolic syndrome (nMetS) subjects or metabolic syndrome (MetS) patients. EVs (MCC-EVs) or cells (MCC-cells) were pre-incubated with MCC950 (1 µg/mL) ($n=8$). (**B**) Transmigration of monocytes through an endothelial cell monolayer induced by EVs from nMetS or MetS patients. EVs (MCC-EVs) or cells (MCC-cells) were pre-incubated with MCC950 (1 µg/mL) ($n=5$). Data are expressed as mean ± SD. Statistical significance was tested with 1-way ANOVA and Tukey post hoc test between all conditions for each panel. $^{**}p<0.01$, $^{***}p<0.001$ and $^{****}p<0.0001$

and IL-18 (Fig. 5A and B; Supplemental Fig. 5B and 5 C). Although both MetS-lEVs and MetS-sEVs enhanced the release of IL-1ß and IL-18 by SMC, only the effects of MetS-lEVs were statistically significant. Preincubation of EVs (MCC-EVs) or SMC with MCC950 (MCC-cells) significantly reduced the effects of MetS-lEVs in IL-1ß and IL-18 release (Fig. 5A and B).

Collectively, these data suggest that MetS-lEVs induce SMC migration, proliferation, and a pro-inflammatory phenotype that could induce SMC remodeling, through a mechanism dependent on NLRP3 inflammasome activation.

NLRP3 associated with MetS-EVs promotes the secretion of pro-inflammatory cytokines in macrophages

The effect of EVs on macrophage activation was analyzed by measuring the secretion in culture cell supernatant of various cytokines and chemokines related to the inflammatory process and vascular remodeling. LPS, but not MCC950, significantly enhanced all cytokine productions (Supplemental Fig. 6A). Treatment with MetS-EVs, but not those from nMetS subjects, significantly increased the release of IL-1ß, IL-18, IL-6, TNF-α, and CCL2 by human monocyte-derived macrophages (MDM) (Fig. 6A-E, Supplemental Fig. 6B and C). Pretreatment of either EVs (MCC-EVs) or the MDM (MCC-cells) with

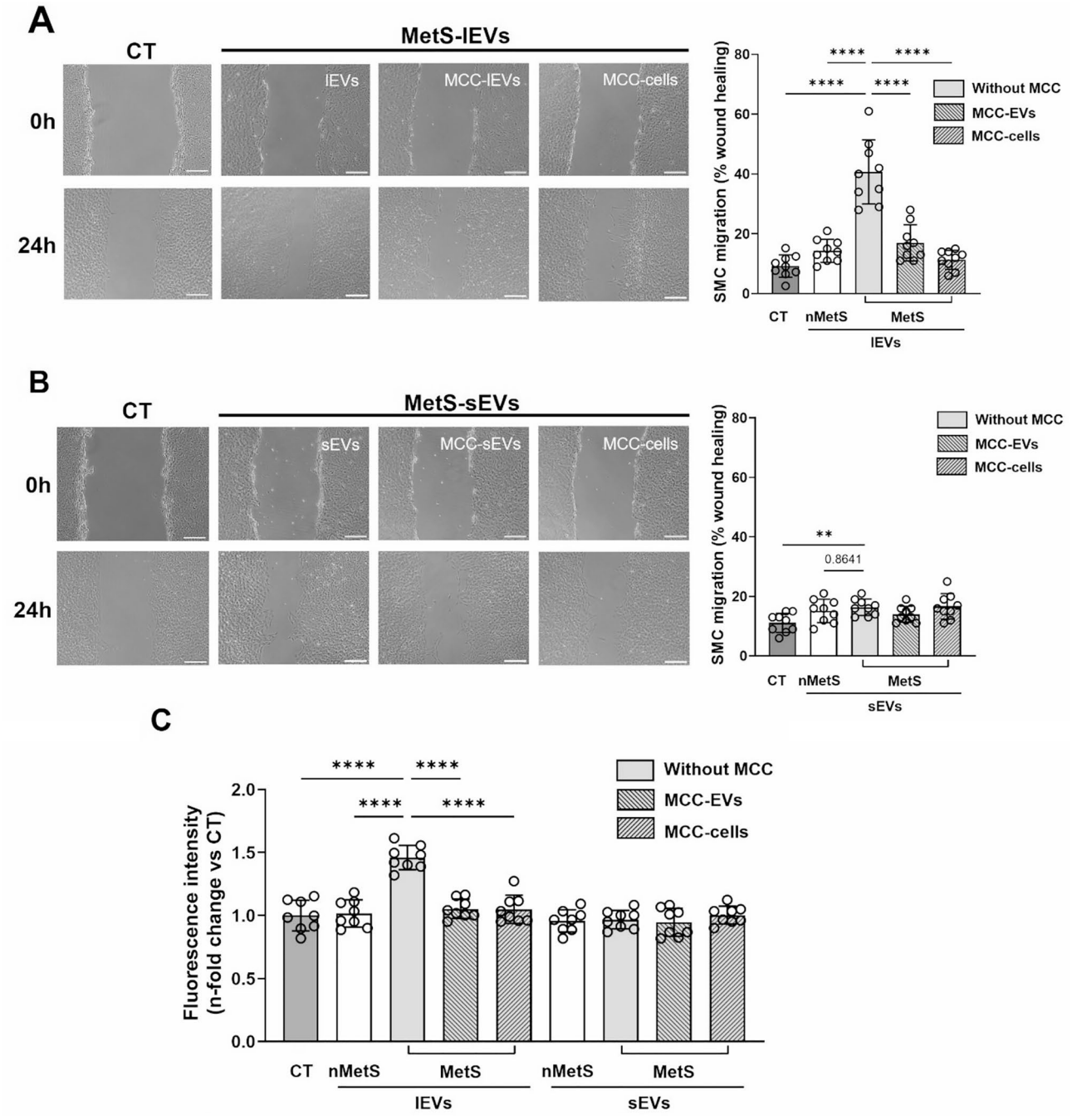

Fig. 4 Effect of NLRP3^{+}-extracellular vesicles (EVs) on smooth muscle cell (SMC) migration and proliferation. (**A** and **B**) Representative microscopy images and quantification of human aortic SMC migration analyzed by wound healing assay at 0 h and after 24 h of treatment with by large EVs (lEVs) or small EVs (sEVs) from non-metabolic syndrome (nMetS) and metabolic syndrome (MetS) patients. EVs (MCC-EVs) or cells (MCC-cells) were pre-incubated with MCC950 (1 µg/mL). White bar = 200 µm. (**C**) Effects of lEVs or sEVs from nMetS and MetS patients on the number of SMC analyzed by CyQuant Kit. EVs (MCC-EVs) or cells (MCC-cells) were pre-incubated with MCC950 (1 µg/mL). Histograms show fluorescence intensity representing the changes in cell number. ($n = 8$). Data are expressed as mean ± SD. Statistical significance was tested with 1-way ANOVA and Tukey post hoc test between all conditions for each panel. Statistical significance: $^{**}p < 0.01$, and $^{****}p < 0.0001$

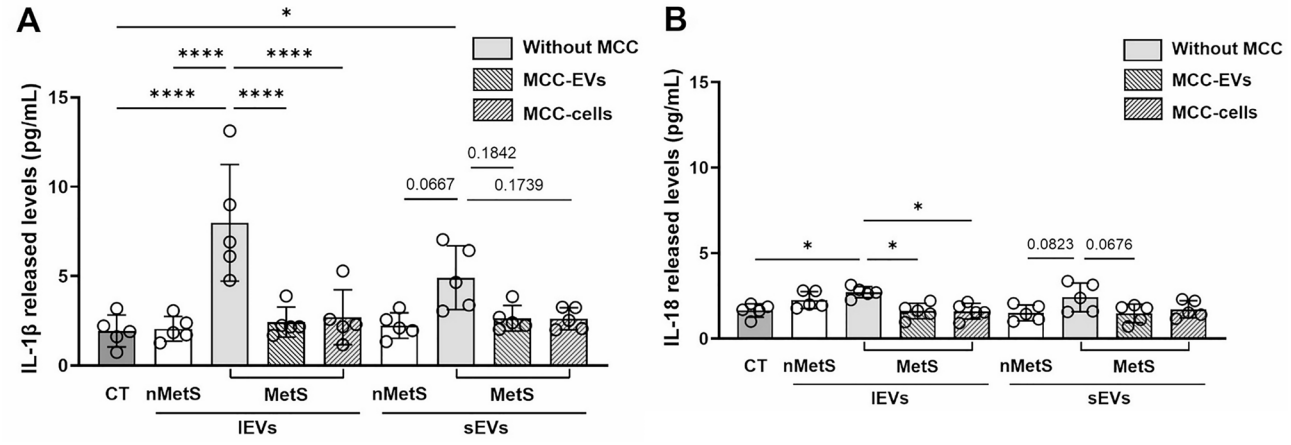

Fig. 5 Role of NLRP3$^+$-extracellular vesicles (EVs) on proinflammatory cytokine secretion by smooth muscle cells (SMC). IL-1ß (**A**) and IL-18 (**B**) production by SMC after 24 h of exposure to lEVs or sEVs from non-metabolic syndrome (nMetS) and metabolic syndrome (MetS) patients. EVs (MCC-EVs) or cells (MCC-cells) were pre-incubated with MCC950 (1 µg/mL) ($n=5$). Data are expressed as mean ± SD. Statistical significance was tested 1-way ANOVA and Tukey post hoc test between all conditions for each panel. *$p<0.05$ and ****$p<0.0001$

MCC950 completely prevented or greatly reduced the release of cytokines, IL-1ß, IL-18, IL-6, TNF-α and CCL2 induced by MetS-EVs (Fig. 6A and E) without affecting the effects of nMetS-EVs (Supplemental Fig. 6B and C). These results suggest that MetS-EVs are critical inflammatory transducers by increasing cytokine and chemokine secretion.

NLRP3$^+$-EVs accumulate in AP and increase endothelial permeability

lEVs were higher in AP samples compared to WAL (Fig. 7A). The analysis of the composition of lEVs isolated from AP and in samples of WAL showed increased levels of Annexin V$^+$-lEVs compared to WAL (Fig. 7B). Further analysis revealed that higher levels of CD4-, CD14-, CD66b-, CD41-, CD144-, CD235a and αSMA-derived lEVs were found in AP samples compared to WAL (Fig. 7C). TEM analysis of WAL- and APlEVs showed no differences in their size (Fig. 7D). sEVs were accumulated to a greater extent in the AP samples compared to the WAL samples (Fig. 7F). In addition, the size of sEVs was smaller in WAL compared to AP by both TEM and NTA analysis (Fig. 7E and F).

A notable finding was the observation that, in contrast to WAL, AP samples exhibited an increased abundance of NLRP3$^+$-lEVs (Fig. 7G). It should be noted that NLRP3$^+$-lEVs are derived from all cell origins examined (Fig. 7H). These results confirm the accumulation of NLRP3$^+$-EVs in human atherosclerotic plaques. Finally, to assess whether AP-EVs have a pathophysiological role, we analyzed their effect on endothelial cell permeability. Both lEVs and sEVs from AP, but not those from WAL, induced a concentration-dependent decrease in TEER (Fig. 7I, Supplemental Fig. 8A and B). These results indicate that EVs accumulated in atheroma increase in vitro endothelial permeability could lead to an alteration in endothelial integrity. These data and the increase on proliferation and migration of SMC induced by MetS-EVs as well as the pro-inflammatory factors secreted by macrophages may collectively contribute to the complication and vulnerability of the atherosclerotic lesions.

Discussion

The present study provides evidence that EVs from MetS patients drive vascular inflammation and several stages of atherosclerosis through the NLRP3-inflammasome pathway. Indeed, NLRP3-inflammasome components were expressed in circulating lEVs and sEVs from MetS patients. Circulating levels of NLRP3$^+$-lEVs correlated with anthropometric and biochemical parameters associated with MetS, including obesity, high diastolic blood pressure, insulin resistance and dyslipidemia, leading to an increased risk of cardiovascular events. At the cellular and molecular level, EVs from MetS patients increased endothelial cell permeability and monocyte transcytosis, induced SMC migration, proliferation, and production of inflammatory cytokines associated with the development of atherosclerosis, especially IL-1ß and IL-18 as well as the release of IL-1ß, IL-18, IL-6, TNF-α and CCL2 from macrophages. These effects of EVs occurred via a MCC950-sensitive mechanism, as described by others [22]. Thus, the expression of both TNF-α and IL-6 was likely the result of IL-1β and IL-18 activation by NLRP3 pathways, which exert a feedback activation of NF-κB. More importantly, by using vascular biopsies from patients undergoing carotid endarterectomy, we showed an accumulation of EVs in atherosclerotic lesions including NLRP3$^+$-lEVs enriched in specific markers related to monocytes, lymphocytes, platelets, granulocytes, endothelial cells, erythrocytes and SMCs. EVs accumulated in

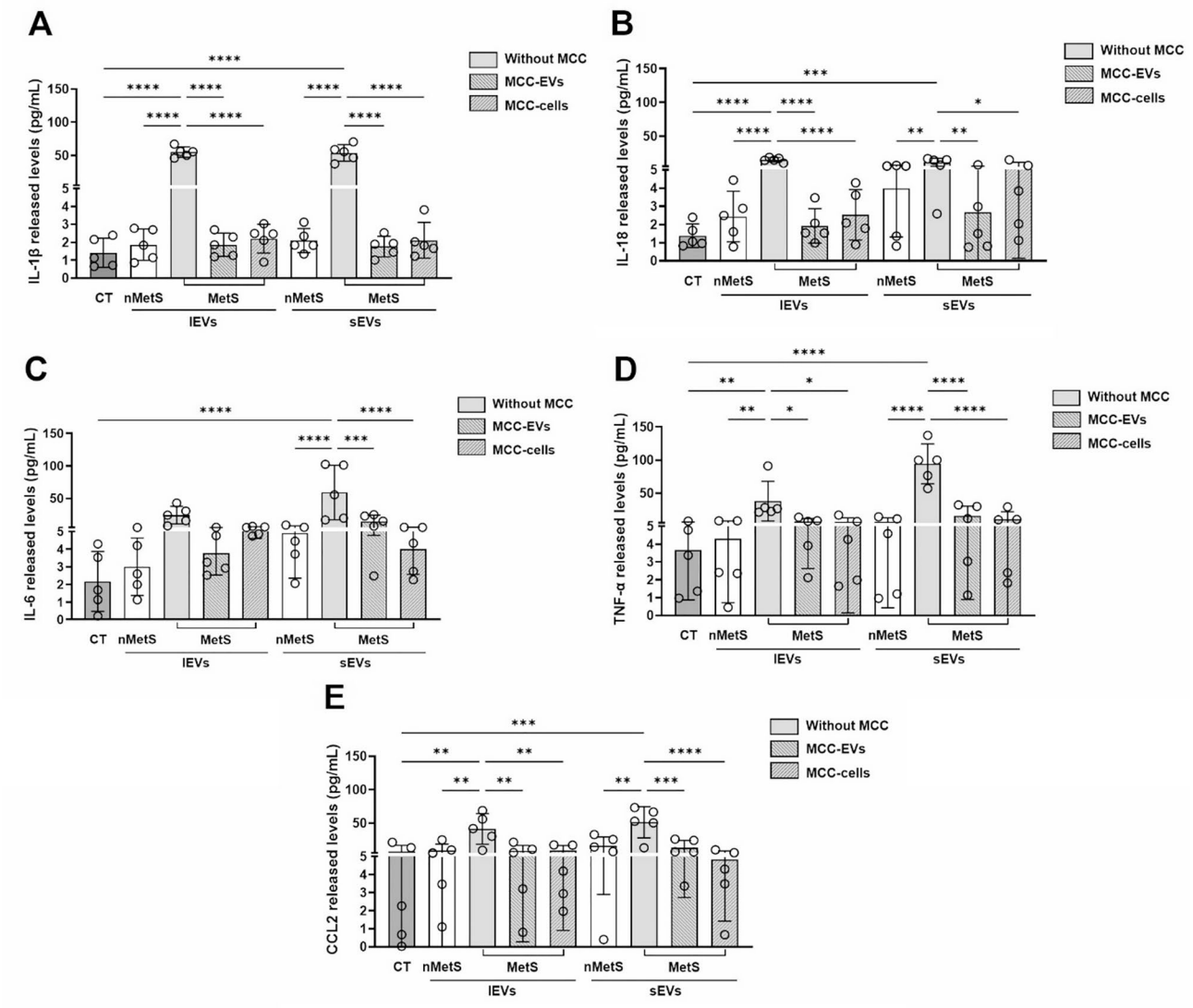

Fig. 6 Effect of NLRP3^{+}-extracellular vesicles (EVs) on macrophage activation. IL-1β (**A**), IL-18 (**B**), IL-6 (**C**), TNF-α (**D**) and CCL2 (**E**) production by human monocyte-derived macrophages after 24 h of exposure to lEVs or sEVs from non-metabolic syndrome (nMetS) and metabolic syndrome (MetS) patients. EVs (MCC-EVs) or cells (MCC-cells) were pre-incubated with MCC950 (1 µg/mL). ($n = 5$). Data are expressed as mean ± SD. Statistical significance was tested with 1-way ANOVA and Tukey post hoc test between all conditions for each panel. *$p < 0.05$, **$p < 0.01$, ***$p < 0.001$ and **** $p < 0.001$

atherosclerotic plaques increased endothelial permeability and might contribute to the complication and vulnerability of the atherosclerotic lesion. Thus, EVs carrying NLRP3 may represent potential biomarkers and targets for novel therapeutic strategies for cardiovascular events related to the inflammatory hypothesis of atherothrombosis. We have recently reviewed that EVs can be potential biomarkers of pathologies associated with obesity, CVD, and diabetes [14, 15]. Here, we showed that both lEVs and sEVs from nMetS and MetS patients expressed all components of the NLRP3-inflammasome including NLRP3, ASC, pro-Caspase-1/Caspase-1, and pro-IL-1ß. Remarkably, NLRP3 and Caspase-1 were overexpressed in MetS-lEVs whereas pro-Caspase-1 and Caspase-1 in MetS-sEVs. Since EV composition reflects the inflammatory state of the originating cell, it is most likely that the NLRP3 inflammasome are present in mother cells, and then, all inflammasome components are incorporated into lEVs via the blebbing of the cell membrane, or into the multivesicular bodies for sEVs. Furthermore, as NLRP3 inflammasome activation has been described in metabolic disorders [9], this may explain the overexpression of several inflammasome components in EVs from MetS patients compared to nMetS. In addition, NLRP3 is present in EVs of all cell origins in lEVs at varying levels of expression. This suggests that the accumulation of inflammasome components in EVs is not a cell-selective process. Also, it is challenging to hypothesize that the NLRP3 inflammasome components are in a form of activated complexes, given that the diameters of

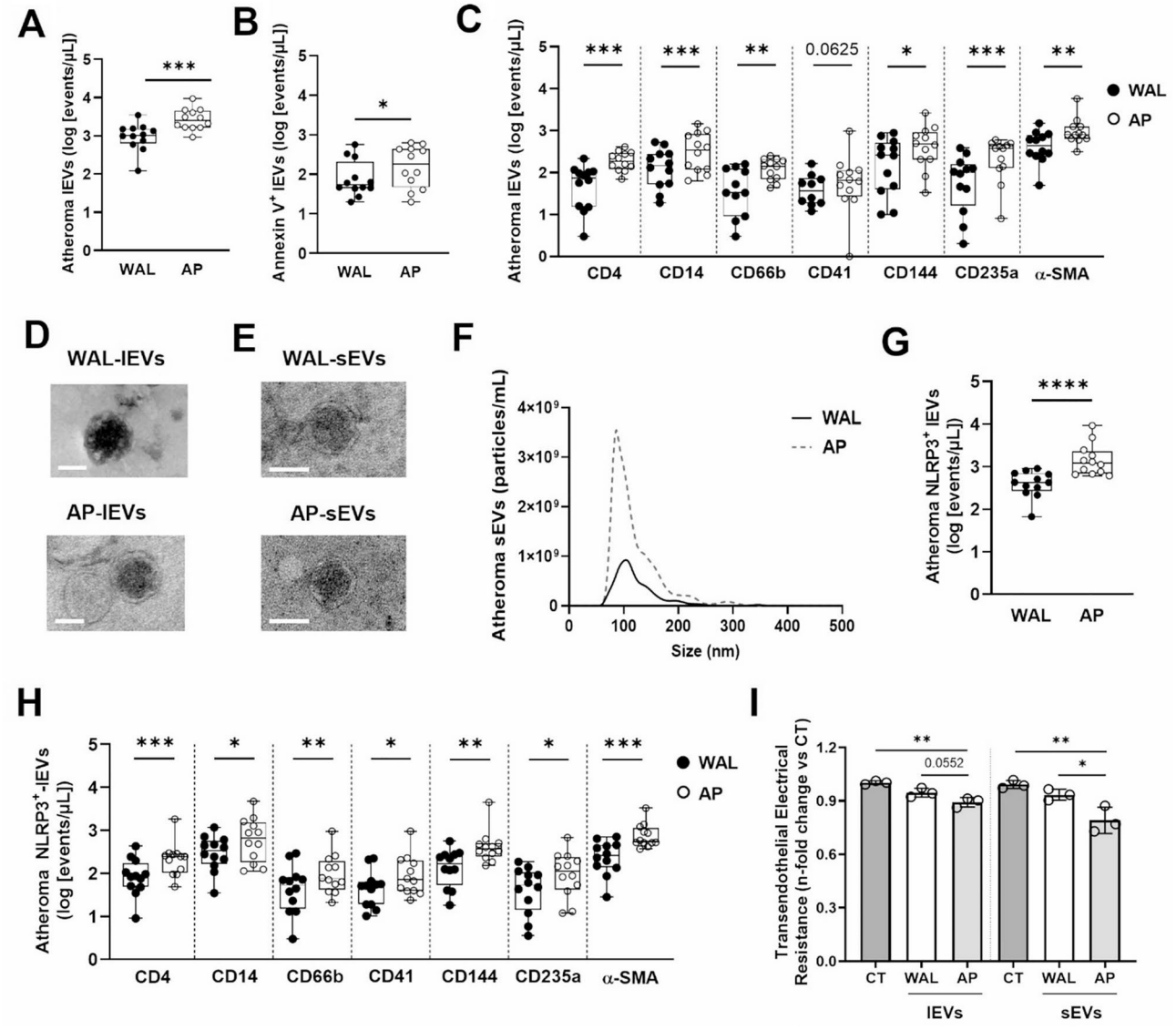

Fig. 7 Characterization of extracellular vesicles (EVs) from human atherosclerotic plaque (AP) from patients undergoing carotid endarterectomy. (**A**-**C**) Quantification of (**A**) total, (B) pro-coagulant (annexin V$^+$) and (**C**) cellular origins of lEVs from wall adjacent to the lesion (WAL-lEVs, full dots) and AP-lEVs (empty dots) ($n = 12$). (**D** and **E**) Representative TEM images of lEVs and sEVs from WAL and AP (scale-bar size: 200 nm and 50 nm for **D** and **E**, respectively). (**F**) Representative NTA analysis for WAL- and AP-sEVs. (**G**-**H**) NLRP3$^+$-lEVs (G) levels and (**H**) cellular origins in WAL- and AP-lEVs ($n = 12$). (**I**) Changes on endothelial permeability induced by WAL- and AP-EVs (20 µg/mL) measured by TEER ($n = 3$). Data are shown as median ± IQR of the log of [lEVs/µL] for **A**, **B**, **C**, **G**, and **H**, and mean ± SD for **I**. Statistical significance was tested with paired Student's t-test, Wilcoxon test, or with 1-way ANOVA and Tukey post hoc test between all conditions for each panel as appropriate. *$p < 0.05$, **$p < 0.01$, ***$p < 0.001$ and **** $p < 0.001$

the specks range from 500 nm to 1 µm [23]. We showed increased circulating levels of NLRP3$^+$-lEVs in MetS patients compared to nMetS subjects including those originating from monocytes, lymphocytes, and activated endothelial cells. It should be noted that neither total-lEVs nor NLRP3$^+$-lEVs correlated with total cholesterol or LDL-cholesterol. This is in line with our previous work on the absence of lipoproteins in MetS-EV samples [19, 24]. Interestingly, circulating lEVs carrying NLRP3 were positively correlated with waist and hip circumference, BMI, glycemia, HbA1c, HDL-cholesterol, plasma triglyceride concentration, and the TyG index and T/HDL-cholesterol ratio which reflect insulin resistance. These results suggest that circulating NLRP3$^+$-lEV levels increase with obesity, insulin resistance, and dyslipidemia. These findings support our previous works [14–19] and reinforce that lEVs expressing NLRP3 may be useful in identifying individuals at high risk of developing atherosclerotic cardiovascular events. Duewell et al. [25] first reported evidence that the NLRP3 inflammasome contributes to the progression of atherosclerosis. Using bone marrow transplanted mice, they showed that a lack

of NLRP3, ASC, or IL-1α/ß in bone marrow cells of atheroprone low-density lipoprotein receptor-deficient mice reduced the atherosclerotic lesion size [25]. The potential role of NLRP3 carried by lEVs as transducers of inflammatory signals leading cardiovascular risk factors to vascular injury has been reported in vitro [20]. Silvis et al. [21] reported that colchicine reduced $CD9^+$/$NLRP3^+$-sEV protein levels in chronic coronary disease. Also, atherogenic stimulation of endothelial cells by oxysterol 7-ketocholesterol induced NLRP3 inflammasome formation and activation, and the secretion of IL-1β-containing EVs that promoted SMC proliferation and migration [26]. Taking together, the present study supports the hypothesis that circulating levels of lEVs harboring NLRP3 may be useful in evaluating atherosclerosis leading to the development of cardiovascular events in MetS patients.

Here, we show that circulating EVs can activate the NLRP3-inflammasome pathway on target cells involved in the progression of atherosclerosis. Both MetS-lEVs and MetS-sEVs, but not those from nMetS subjects, increased endothelial permeability and monocyte transmigration by a mechanism sensitive to pharmacological inhibition of NLRP3 with MCC950. It is interesting to indicate that MetS-sEVs induced an increase of endothelial permeability although the expression of NLRP3 in these samples was not significantly increased when compared to nMetS-sEVs. This may be explained by the fact that other components of the inflammasome such as pro-Caspase-1 and Caspase-1 are increased. Consequently, the formation of the active form of the inflammasome, the speck, may be prevented by blocking NLRP3 with MCC950, as the assembly of its components is dependent on this process. Thus, NLRP3 and inflammasome components carried by EVs activated the NLRP3-inflammasome pathway and disrupted endothelial integrity which is the first step in atherosclerosis.

In primary human aortic SMC, we found that MetS-lEVs, but not MetS-sEVs, increased migration, proliferation, and IL-1ß and IL-18 secretion via a mechanism sensitive to pharmacological inhibition of NLRP3. Activation and recruitment of NLRP3 to assemble the inflammasome complex is the causal mechanism associated with increased levels of proinflammatory cytokine secretion, mainly in macrophages [27, 28]. The present study showed that MetS-lEVs and MetS-sEVs, but not nMetS-lEVs and nMetS-sEVs, significantly increased the levels of IL-1ß, IL-18, IL-6, TNF-α, and CCL2 in the macrophage supernatant. These effects were either prevented or markedly reduced by pharmacological blockade of NLRP3 with MCC950. These results support that MetS-EVs are critical drivers of inflammation by increasing SMC and macrophage secretion of cytokines and chemokines related to atherosclerosis development.

Besides, we found that both types of EVs accumulated in atherosclerotic lesions from humans undergoing carotid endarterectomy and increased endothelial permeability and thus compromised endothelial integrity. Furthermore, human atherosclerotic plaques were enriched in $NLRP3^+$-lEVs originated from monocytes, lymphocytes, platelets, granulocytes, endothelial cells, erythrocytes, and SMCs. These results confirm the accumulation of NLRP3-carrying EVs in human atherosclerotic plaques and strengthen our hypothesis that circulating $NLRP3^+$-lEVs play a role in the development of atherosclerosis and their contribution to the complication and vulnerability of human atherosclerotic lesions.

The mechanisms by which $NLRP3^+$-EVs from MetS act on target cells are likely to be due to the uptake of EVs by recipient cells and subsequent transfer of EV-encapsulated NLRP3-inflammasome components into the cells. Indeed, we have reported that sEVs from MetS were internalized by endothelial cells 4 h after treatment. sEVs from nMetS and MetS patients showed similar localization around the nucleus of human aortic endothelial cells after 24 h of treatment [17]. We also previously found that lEVs from nMetS and MetS patients were internalized by human primary aortic SMCs [19]. Here, we showed that all types of EVs were internalized in endothelial cells, SMC and macrophages indicating a common mechanism independent of the cell target (Supplemental Figs. 7A to C). In addition, internalization of EVs was not modified in the presence of MCC950 suggesting that the abolition of effects induced by MetS-EVs was due to the direct action of MCC950 on NLRP3 pathway rather a decrease on EV internalization (Supplemental Figs. 7A to C). Thus, it is likely that $NLRP3^+$-lEVs and $NLRP3^+$-sEVs mediate their effects through transfer of the NLRP3-inflammasome components via internalization of these EVs on target cells including endothelial cells, SMCs and macrophages. The present study demonstrates that, in the absence of the classical mechanism of priming and activation, NLRP3-inflammasome components delivered by EVs on target cells are capable of assembling to form the complex NLRP3-ASC speck. As shown by others, LPS alone induced increase in the expression levels of NLRP3, ASC and Caspase-1 in human gingival epithelial cells [29] or trophoblasts [30]. This assembly might be triggered by the increasing intracellular ROS levels induced by other cargos in MetS-EVs. Our previous studies described the existence of such cargos, including Fas-FasL pathways by MetS-lEVs and LPS-TLR4 pathways by MetS-sEVs [17, 18]. In addition, MetS-lEVs and MetS-sEVs could potentially increase the recruitment of proinflammatory circulating cells, such as leukocytes, under conditions associated with vascular inflammation. The role of exogenous (i.e. carried by EVs) *versus* endogenous (within target cells) NLRP3-inflammasome

activity in vitro can be questioned because the effects of either lEVs or sEVs from MetS were abolished not only when NLRP3 was inhibited into EVs (MCC-EVs), but also when NLRP3 was inhibited within cells (MCC-cells). These findings may be attributed to the fact that when MCC950 is employed to inhibit NLRP3 on target cells, the inhibitor remains within the cells and can also inhibit exogenous NLRP3 carried by EVs. In addition, MCC950 had no effect on the response of either lEVs or sEVs from nMetS patients, suggesting that a specific quantity of NLRP3 inflammasome components is indispensable for the generation of adequate levels of IL-1β and IL-18, and, consequently, the MCC950 treatment exhibited no impact on the EVs from nMetS individuals. Also, these experiments exclude that the effects observed are due to the LPS carried by MetS EVs [17] since MCC950 strongly inhibited or abrogated the effects of either lEVs or sEVs from MetS. Collectively, these findings suggest that the effects of MetS-EVs are predominantly driven by exogenous NLRP3 carried by EVs. In this context, MCC950 was reported to be the most specific against NLRP3 and when administered to apolipoprotein E-deficient mice inhibited NLRP3 expression with a significant reduction in the atherosclerotic plaque area, independent of lipid profile [31]. In humans, this drug may potentially prevent diseases associated with the NLRP3 inflammasome, including small vessel disease, stroke in diabetic patients, and other CVDs [32].

Finally, the effects of EVs from MetS on different steps of SMC-related atherosclerosis development are mainly driven by lEVs but not by sEVs. Several hypotheses can be advanced to explain the observed discrepancies between MetS-lEVs and MetS-sEVs. First, although both types of EVs carried different components of the NLRP3 inflammasome, only lEVs from MetS showed higher protein expression of NLRP3 compared to nMetS EVs, whereas NLRP3 expression was similar in sEVs from MetS and nMetS subjects. Second, we have recently reported that Rap1 carried by lEVs from MetS patients induces SMC proliferation, migration, and secretion of proinflammatory cytokines [19]. It has recently been reported that Rap1 signaling is associated with IL-1β production in peripheral blood mononuclear cells of systemic inflammation in epileptic patients [33]. Since lEVs from MetS, but not sEVs (see Supplemental Fig. 1F) exhibited Rap1 expression, it may be possible that Rap1 is involved in the increased expression of NLRP3 observed in MetS lEVs, thereby triggering the ability of lEVs to play a critical role in the processes involved in SMC remodeling.

Limitations: A limitation of this study is the unknown mechanism by which EVs from MetS patients are enriched in NLRP3, but also in other inflammasome components, should be addressed, and this could be due to dyslipidemia, insulin resistance, and inflammatory processes. Despite these limitations, the present translational study demonstrates that $NLRP3^+$-EVs can be potential biomarkers and play a significant role in the inflammatory process leading to atherosclerosis. Additionally, it should to be noted that cultured cells were exposed to EVs at the circulating concentrations for each subject, being the physiological concentration for the vascular endothelium but probably overestimated for SMC and macrophages. Also, the present study reinforces the hypothesis that inhibiting the NLRP3-inflammasome pathway reduces the risk of atherosclerotic CVD. On the other hand, longitudinal studies should be undertaken to test whether treatment of NLRP3 inhibitors or IL-1ß inhibitors would decrease circulating $NLRP3^+$-EV levels or their activities in MetS patients, reduce inflammation and prevent atherosclerosis. Also, the present manuscript focused on cellular phenotypes rather than directly examining atherosclerotic plaque formation or progression in vivo. The observation of plaque formation and progression in apolipoprotein E-deficient mice necessitates a minimum of 12 weeks of feeding the animals a high-fat diet. Due to the limited quantity of EVs that can be isolated from patients, it is not feasible to obtain a sufficient amount of EVs to conduct such experiments, which require a minimum of 12 weeks of in vivo injection. Nevertheless, cultured cells were exposed to EVs at the circulating concentrations for each subject, being the physiological concentration for the vascular endothelium but probably overestimated for SMC and macrophages. Moreover, we reported that NLRP3-EVs modulated in these appropriated cultured cells all the steps leading to the early state of atherosclerosis. Finally, injection of these EVs in mice for two weeks resulted in impaired systemic, adipose tissue, and liver insulin signaling as well as the development of obesity which is a major contributing factor to plaque formation and progression in vivo [24]. Altogether, the findings of this study provide compelling evidence to support the conclusion that circulating $NLRP3^+$-EVs play a significant role, at least in the initial stage of atherosclerosis, and that they contribute to the complexity and susceptibility of human atherosclerotic lesions.

In conclusion, we demonstrate that, in MetS, NLRP3 carried by EVs is actively involved in the development of atherosclerosis and in the complications of atherosclerotic lesions. Furthermore, our results indicate that circulating EVs carrying NLRP3 can be proposed as potential biomarkers to predict the vascular consequences of MetS.

These findings highlight the important role of EVs in atherosclerotic CVD and add novel targets in addition to our previous findings showing that: (i) MetS-EVs induce endothelial dysfunction either through activation of the Fas/FasL- or TLR4- for lEVs [16, 18] and sEVs

[17], respectively and (ii) MetS-lEVs carrying Rap1 are involved in vascular inflammation and remodeling, and atherosclerosis [19]. Finally, inhibition of the NLRP3-inflammasome may be an effective therapeutic strategy for secondary prevention in patients at high-risk of cardiovascular events.

Methods

Our study examined male and female human subjects. Similar findings are reported for both sexes. Data, analytic methods, and study materials for the purposes of reproducing the results or replicating procedures can be made available on request to the corresponding author who manages the information.

Patients

Non-MetS (nMetS) and MetS patients were recruited at the Department of Endocrinology and Nutrition of the University Hospital of Angers in accordance with the Declaration of Helsinki. After giving their informed written consent, all participants were characterized according to the unified criteria for MetS proposed by the International Diabetes Federation [2]. Briefly, subjects were identified as having MetS if they had at least three of the following five criteria: (i) waist circumference > 102–88 cm for men and women, respectively; (ii) systolic and diastolic blood pressure ≥ 130/85 mmHg or on pharmacological treatment in patients with a history of hypertension; (iii) fasting glycemia ≥ 1.0 g/L or on pharmacological treatment for elevated glucose; (iv) triglycerides ≥ 1.5 g/L or on pharmacological treatment for elevated triglycerides; and (v) HDL-cholesterol < 0.4 g/L in men or < 0.5 g/L in women, or on pharmacological treatment for reduced HDL-cholesterol. Patients with pre-existing chronic inflammatory diseases or cancer were excluded from the present study. A total of 26 subjects were identified as MetS patients and 23 subjects with two or less MetS criteria were identified as nMetS subjects. Baseline characteristics and clinical data of nMetS and MetS subjects are summarized in Table 1.

EV isolation from peripheral blood

Peripheral blood (25 mL) from nMetS and MetS patients was collected in ethylene-diamine-tetraacetic acid tubes (Vacutainers; Becton Dickinson, Le Pont de Claix, France) to isolate circulating EVs as previously described [16, 17, 19, 24]. Briefly, platelet-rich plasma was separated from whole blood after centrifugation at 260 x *g* for 15 min and then centrifuged at 1,500 x *g* for 20 min to obtain platelet-free plasma (PFP). Two hundred microliters of PFP were frozen and stored at -80 °C until subsequent use. The remaining PFP was used to purify both types of EVs by sequential high-speed centrifugation. First, PFP was centrifuged at 17,000 x *g* for 45 min to collect lEVs. The lEVs were then washed with 0.9% NaCl solution and recentrifuged at 17,000 x *g* for 45 min. The supernatant was replaced with 200 µL NaCl and stored at + 4 °C. On the other hand, lEV-depleted plasma was centrifuged at 100,000 x *g* (Optima MAX-XP ultracentrifuge and MLA-80 rotor, Beckman Coulter, Villepinte, France) for 70 min to pellet sEVs. The sEVs were then washed in phosphate-buffered saline (PBS) (NaCl 137 mM, KCl 2.7 mM, Na_2HPO_4 10 mM, KH_2PO_4 1.8 mM, pH = 7.4) and recentrifuged at 100,000 x *g* for 70 min. Finally, sEVs pellet was resuspended in 200 µL of PBS and stored at + 4 °C until further use.

EV characterization

Following the recommendations of MISEV 2024 guidelines about plasmatic lEVs and sEVs characterization, different analyses were performed to validate the isolation and purity of EV subtype preparations including differential light scattering, flow cytometry, nanotracking analysis, electronic microscopy, and immunoblot of specific EV markers [34].

Differential light scattering

After EV isolation, 10 µL of purified lEVs and 5 µL of purified sEVs were diluted in 990 µL and 995 µL of filtered 1X PBS, respectively, and then vortexed for 1 min to avoid EV aggregation. Each sample was immediately put in disposable cuvette for the analysis. Using a Zetasizer Nano ZS (Malvern Instruments, Malvern, UK), the size of EVs was analyzed in terms of mean size (Z-average) of the particle distribution and homogeneity (PDI). The limitations of Zetasizer technique in detecting protein markers of EVs preclude the quantification of NLRP3 expression on these EVs. All results were obtained from three independent measurements (three runs for each measurement at + 25 °C) followed by data analysis and processing which were carried out with the help of the Zetasizer software, version 7.03.

Phenotyping of NLRP3-carrying lEV

Numeration and phenotyping of the lEVs were performed by flow cytometry of PFP. An example of the gating strategy used for this type of analysis is shown in Supplemental Fig. 1. Regions corresponding to total lEVs were identified in FSC and SSC intensity dot plot representation set at logarithmic gain, depending on their diameter (0.1–1 µm). The percentages show the number of positive events for staining of circulating lEVs visualized by plotting NLRP3 marker (x-axis) versus total events (y-axis) and gated based on isotype control.

Cell origin analysis of lEVs was performed according to the expression of membrane-specific antigens, as previously described [16, 19]. The following antibodies were used: anti-CD41-PC5, anti-CD144-PE,

anti-CD66b-FITC, anti-CD4-FITC, anti-CD235a-FITC (Beckman Coulter) and anti-CD14-PCy7 (BioLegend, San Diego, CA). Since NLRP3 is located inside EVs, they were fixed with a 2% paraformaldehyde for 15 min, centrifuged at 17,000 x *g* for 45 min at +4ºC, and permeabilized with a 0.1% saponin solution in PBS for 5 min prior to rabbit anti-NLRP3 antibody (Cell Signaling, Boston, MA) incubation. Then, lEVs were labeled with donkey anti-rabbit FITC (Invitrogen, Waltham, MA) or Alexa Fluor 555 (Abcam, Cambridge, UK) secondary antibody. Because no labelling of NLRP3 was observed when lEVs were not permeabilized, further analysis of NLRP3 was performed on permeabilized lEVs (Supplemental Fig. 1). To evaluate the cellular origin of NLRP3-lEVs, specific cell markers were co-labelled with NLRP3 in permeabilized lEVs. Also, for α-smooth muscle actin labelling, lEVs were incubated with anti-alpha smooth muscle actin antibody (Invitrogen) after permeabilization with saponin and labelled with Alexa Fluor 555 (Abcam, Cambridge, UK) secondary antibody. Irrelevant human IgG was used as an isotype-matched negative control for each sample. After 45 min of incubation with antibodies, flow-count microbeads (Beckman Coulter) were added to count the lEVs of each sample, and then the samples were analyzed by flow cytometry (500 MP System, Beckman Coulter).

Nanoparticle tracking analysis (NTA) for sEV characterization

sEV samples were diluted in 0.22 µm filtered NaCl prior to the NTA measurements (NanoSight NS300, Malvern Instruments Ltd., Malvern, UK) equipped using a 405 nm laser. Five videos of 60 s each were recorded per sample using optimized set parameters. The temperature was automatically controlled and ranged from +20 °C to +21 °C. Videos were analyzed when enough valid trajectories were measured. The results correspond to the mean of the videos recorded for each biological sample. sEV concentrations were normalized by the collected plasma volume for each patient. Data acquisition and further analysis were performed using the NTA software version 3.1.

Transmission electronic microscopy

EV preparations were first fixed overnight at +4 °C with 2.5% glutaraldehyde (LFG Distribution, Lyon, France) in 0.1 M PBS. The EVs were then washed twice in PBS centrifugation at 100,000 x *g* for 70 min. EVs were resuspended in Milli-Q water, and 20 µL were applied to Formvar®-coated copper grids for 2 min. EVs were negatively stained with 20 µL of uranyl acetate 5% (diluted in 50% ethanol) for 30 s. The grids were then briefly rinsed with Milli-Q water and left to air dry. The grids were then observed with a Jeol JEM 1400 microscope (Jeol, Croissy Sur Seine, France) operating at 120 keV.

Immunoblots

Ten µg of total EV proteins were separated by electrophoresis on 4–20% Tris-Glycine Precast gels (Biorad, Hercules, CA) and then transferred to nitrocellulose membranes using the Turbo Transblot system (Bio-Rad). membranes were incubated overnight at +4 °C with the following primary antibodies from Santa Cruz Biotechnology (Dallas, TX) (anti-CD9, anti-CD63, anti-TSG-101), Cell Signaling (Boston, MA) (anti-Rap1, anti-NLRP3, anti-ASC, anti-Caspase-1 and anti-pro-IL-1β).

The membranes were then incubated with the appropriate horseradish peroxidase-conjugated secondary antibodies (Cell Signaling). Protein-antibody complexes were detected using SuperSignal™ West Femto Maximum Sensitivity Substrate (Thermo Scientific, Waltham, MA). In some experiments, IRDye 680RD and 800CW anti-mouse IgG H + L secondary antibodies were used for fluorescence detection of proteins. Detection was performed using an Odyssey Fc Imaging System (LI-COR). All membranes were re-blotted using a monoclonal antibody against β-actin (Sigma Aldrich) and anti-CD81 (Santa Cruz Biotechnologies) as loading controls for lEVs and sEVs, respectively. Densitometric analyses of Western blots were performed using ImageJ software, and data were normalized to the corresponding total protein expression.

Cell models

Primary human aortic ECs (HAoEC, Promocell, Heidelberg, Germany) were cultured in EC growth medium MV2 (Promocell) supplemented with endothelial growth factors and 1% penicillin-streptomycin (Sigma-Aldrich, Saint-Louis, MI).

Human aortic SMC were obtained by enzymatic dissociation and pooled from the non-atherosclerotic abdominal aortas of five organ donors without cardiometabolic diseases or risk factors. Collection, storage and use of tissue were performed following the principles outlined in the Declaration of Helsinki and approved by the local Ethics Committee in accordance with Spanish legal regulations, as previously described [35, 36]. Informed written consent was obtained from each donor. Human aortic SMC were cultured in Dulbecco's modified eagle medium (DMEM) low glucose medium (Sigma-Aldrich) supplemented with 10% sEV-deprived fetal bovine serum (FBS) and 1% penicillin-streptomycin. sEV-deprived FBS was obtained by centrifugation at 200,000 x *g* for 130 min at +4 °C, and filtered at 0.22 µm.

Primary human MDM were obtained after CD14 positive selection of monocytes from buffy coats obtained from the French Establishment of Blood (EFS, Angers). Peripheral blood mononuclear cells were isolated by Histopaque-1077 (1.077 g/L, Sigma-Aldrich) density centrifugation and monocytes were selected using

CD14-specific magnetic beads (Miltenyi Biotec, Bergisch Gladbach, Germany). $CD14^+$-selected cells were resuspended in RPMI-1640 medium supplemented with 10% sEV-depleted FBS, 1% penicillin-streptomycin, 1% sodium pyruvate, 1% L-glutamine, and 1% non-essential amino acids (all for Sigma-Aldrich).

lEVs from nMetS or MetS subjects were used at the circulating concentration determined for each individual, as previously described [16, 17, 19]. The values of circulating lEVs detected in the donors ranged from 4,825 and 81,260/µL of plasma for nMetS and 10,553 and 236,077/µL of plasma for MetS patients. The same volume of the supernatant from the last centrifugation step was also used as control (CT). As used in previous studies, the chosen working concentration of sEVs for the experiments was 10 µg of proteins/mL, which ranged from 1.31×10^7 to 6.65×10^9 and from 1.01×10^9 to 25.9×10^9 sEVs/mL of circulating sEVs for nMetS subjects and MetS patients, respectively [17].

Two protocols were used to inhibit either NLRP3 carried by EVs or endogenous NLRP3 in cells. Briefly, for the treatment of EVs, both types of EVs were pre-incubated with 1 µmol/L MCC950 (MCC-EVs) for 30 min at +4 °C. lEVs were pelleted by centrifugation at 21,000 x *g* for 45 min at +4 °C and resuspended in complete media, whereas 30 µL of Exo-Quick solution (System Biosciences) were added to sEVs and the mixture was placed on ice for 30 min before being pelleted by centrifugation at 21,000 x *g* for 3 min and resuspended in complete media. For the second protocol, cells were pre-incubated with the pharmacological NLRP3 inhibitor MCC950 (1 µmol/L) for 30 min before treatment with EVs for 24 h (MCC-cells).

EV interaction with target cells

Purified lEVs and sEVs were stained with PKH67 dye (Sigma-Aldrich), as previously described [17, 19]. In order to stop staining, an equal volume of FBS was added. Then, lEVs were centrifuged at 21,000 x *g* for 45 min, and sEVs at 100,000 x *g* + 4 °C for 70 min to remove the supernatant. Pellets were washed with 0.9% saline salt solution to eliminate the excess of dye. PKH67-labeled EVs were incubated with HAoEC, SMC and MDM for 4 h at 37 °C, in open µ-slide chambered coverslip with 8-well plates (Ibidi GMBH, Martinsried, Germany). At the end of the incubation with EVs, the culture medium was removed, and the cells were washed with 0.9% saline solution. Cells were fixed with 2% paraformaldehyde for 20 min and stained with 0.2U of Alexa Fluor 568-labelled Phalloidin (Thermofisher) diluted in PBS with 1% BSA for 60 min at room temperature. After washing with PBS, nuclei were stained with 6-diamidino-2-phenylindole (DAPI, Santa Cruz Biotechnology). Finally, cells were mounted and visualized using a 63x objective (Plan-Apochromat 63x/1.4 Oil DIC M27) with a confocal microscopy (LSM800, Zeiss, ZEN software).

Trans-epithelial electric resistance (TEER) measurement

HAoECs were seeded at 2.5×10^5 cells/Transwell (0.4 µm pore size, Sarstedt) in the upper chamber and grown to 100% confluence. TEER measurement was performed before pre-incubation with the inhibitor and after 24 h of EV treatment, using a Millicell® ERS-2 Voltohmmeter (Merck, Darmstadt, Germany) to assess endothelial barrier integrity. Measurements were taken at three different points in each well and the mean was calculated.

Monocyte transmigration assay

$CD14^+$-selected cells (3×10^5 cells) were stained with 2 µmol/L of PKH-67 dye in 0.9% NaCl for 2 min at room temperature, according to the manufacturer's instructions (Sigma-Aldrich). Primary monocytes were added to the HAoEC monolayer that was in the upper chamber of the Transwell (8 µm pore size, Sarstedt) and $CD14^+$-cells were allowed to transmigrate for 24 h. The medium of the lower chamber was harvested, centrifuged at 500 x *g* for 10 min to pellet the cells, and resuspended in 200 µL of NaCl. PKH-67-stained monocytes were then counted by flow cytometry.

Wound healing assay

Human aortic SMCs were cultured in DMEM low-glucose medium to 100% confluence. The cells were then serum-starved overnight. The experimental medium was composed of 0.5% FBS-DMEM low glucose supplemented with 2% bovine serum albumin (BSA, Sigma Aldrich). The confluent monolayer was scratched with a sterile 100 µL pipette tip, and cells were gently washed with PBS. Then, fresh medium was added, and the cells were stimulated for 24 h with the EVs preincubated or not with MCC950 inhibitor, as described above. Wound healing closure was monitored by phase contrast microscopy at 0 and 24 h. The percentage of wound healing closure at different time points relative to time 0 was quantified using Image J analysis software (National Institute of Health).

SMC proliferation assay

The CyQUANT® cell proliferation assay kit (Invitrogen, Carlsbad, CA) was used to analyze proliferation. Human aortic SMC were seeded into 96-well plates at a density of 2×10^3 cells per well. They were allowed to attach overnight. Cells were serum starved 4 h prior to their stimulation for 24 h with EVs pre-incubated with or without NLRP3 inhibitor, as described above. The experimental medium consisted of 10% FBS-DMEM low glucose supplemented with 2% BSA. After 24 h, the experimental medium was removed, the dye-binding solution was

added to each microplate well and the cells were incubated at + 37 °C for 30 min. Fluorescence levels were read using a fluorescence microplate reader (485 nm excitation and 530 nm emission, Synergy HT, Biotek, Winooski, VT).

ELISA cytokines multiplex

The secretome of SMC and hMDM was analyzed in cell culture supernatant after 24 h exposure to nMetS and MetS-EVs in the absence or presence of MCC950 inhibitor. Supernatants were recovered and rapidly frozen in liquid nitrogen, and stored at -80 °C until their analysis. A multiplex electrochemiluminescence immunoassay kit (V-PLEX, Meso Scale Discovery, Rockville, MD) was used to measure cytokine concentrations in cell culture supernatant according to the manufacturer's instructions. The pre-coated antibodies allowed the simultaneous quantification of the following cytokines IL-1β, IL-18, IL-6, chemokine (C-C motif) ligand 2 (CCL2) and tumor necrosis factor-alpha (TNF-α). Samples were run in duplicate, plates were read using a Sector Imager 2400 (Meso Scale Discovery) and data were analyzed using Discovery Workbench 4.0 software (Meso Scale Discovery). All MDM samples were within the detection range for all cytokines; however, IL-6, CCL2 and TNF-α levels were not detected in SMC supernatants.

EVs from human atherosclerotic plaque

Human carotid artery plaques were collected from 12 male subjects that underwent carotid endarterectomy surgery. Carotid samples are considered as surgical waste following French ethical laws (L.1211-3 to L.1211-9), in compliance with the Declaration of Helsinki. All carotid samples were obtained from patients with their informed written consent. EV isolation from 7arotid artery plaques was performed as previously described [19, 37]. Briefly, human atheroma samples were rapidly rinsed in cold sterile PBS supplemented with 100 U/ml streptomycin and 100 U/ml penicillin, and the atherosclerotic lesions (AP) were separated from the apparently healthy vessel wall adjacent to the lesion (WAL). Plaques were then thoroughly minced with fine scissors in a volume of fresh DMEM (supplemented with 10 µg/mL polymyxin B, 100 U/mL streptomycin and 100 U/mL penicillin and filtered through a 0.22 µm membrane) equal to 10 times the weight of each lesion to suspend EVs. The resulting preparations were centrifuged first at 400 x *g* (15 min) and then at 12,500 x *g* (5 min) to completely remove cells and cell debris, as previously described [19]. Two hundred µL of the resulting supernatants were used for flow cytometry experiments to measure total lEV levels, NLRP3 expression and phenotype of lEVs as described above. lEVs were pelleted by two centrifugations at 21,000 x *g* (45 min) before being resuspended in 200 µL of 0.9% NaCl. The supernatant depleted in lEVs was centrifuged at 200,000 x *g* (130 min) to pellet sEVs. After a second centrifugation under the same conditions, sEVs were resuspended in 200 µL filtered PBS and stored at + 4°C. The size and number of lEVs and sEVs in AP and WAL samples were analyzed by flow cytometry and NTA, respectively, as described above.

Statistical analysis

Normality of the data was assessed using the Shapiro-Wilk test. Comparisons were made between all conditions for each panel. Statistical analysis was performed using 1-way ANOVA followed by Tukey post-hoc test for multiple comparisons. In cases where normality was not confirmed, statistical analyses of two groups were analyzed by Mann-Whitney U test. Experiment-wide multiple testing correction was not applied. Correlations were performed using the Spearman correlation test. Values presented in text and figures are mean ± standard deviation (SD) or median [IQR] for clinical data and flow cytometry analysis. All P values are shown in tables. In figures, only P values < 0.1 are shown as asterisk ($p < 0.05$) or numbers (p between 0.05 and 0.1). Statistical analysis was performed with GraphPad Prism (version 10.0; GraphPad Software Inc., San Diego, CA).

Abbreviations

And acronyms

AP	atherosclerotic plaque
BMI	body mass index
CCL2	chemokine (C-C motif) ligand 2
CVD	cardiovascular diseases
EVs	extracellular vesicles
HbA1c	glycated hemoglobin
HDL	high-density lipoprotein
HOMA	homeostasis model assessment
IL	interleukin
LDL	low-density lipoprotein
lEVs	large extracellular vesicles
LPS	lipopolysaccharide
MCC950	N-(1,2,3,5,6,7-hexahydro-s-indacen-4-ylcarbamoyl)-4-(2-hydroxypropan-2-yl)furan-2-yl)sulfonylazanide
MDM	monocyte-derived macrophage
MetS	metabolic syndrome
nMetS	non-metabolic syndrome
NTA	nanotracking analysis
sEVs	small extracellular vesicles
SMC	smooth muscle cells
TEER	transendothelial electric resistance
TNF-α	tumor necrosis factor alpha
WAL	wall adjacent to the lesion

Supplementary Information

The online version contains supplementary material available at https://doi.org/10.1186/s12964-025-02296-8.

Supplementary Material 1

Supplementary Material 2

Acknowledgements
We thank S. Marechal-Girault and P. Vandeputte for analysis of clinical data of NUMEVOX cohort. The manuscript and the English have been proof-read by Dr Edward Milbank, Research Associate from the Institute for Diabetes and Obesity, Helmholtz Zentrum München, Neuherberg, Germany.

Author contributions
RA conceptualized and supervised the study. XV-G, LV and MMP conducted experiments and acquired data. XV-G analyzed data. SD, FG, SH, RV, OM and CP provided resources. XV-G and RA found the financial source. XV-G and RA wrote the original draft of the manuscript, which was reviewed and edited by CM, and given final approval by RA.

Funding
This work was supported by INSERM, Université d'Angers and CHU Angers. X. Vidal-Gómez was supported by Fondation pour la Recherche Médicale (SPF201809006985). This work was also supported by the French Federation of Cardiology.

Data availability
No datasets were generated or analysed during the current study.

Declarations

Competing interests
The authors declare no competing interests.

Author details
[1]PhyMedExp, University of Montpellier, INSERM, CNRS, Montpellier, France
[2]SOPAM, INSERM U1063, UNIV Angers, SFR ICAT, Angers, France
[3]CHU d'Angers, Angers, France
[4]Groupe Clinifutur, Clinique Sainte-Clotilde, Sainte-Clotilde, France
[5]DéTROI, INSERM U1188, Université de La Réunion, La Réunion, France
[6]Department of Pharmacology, Medicine School, Autonomous University of Madrid, Madrid, Spain

Received: 23 January 2025 / Accepted: 7 June 2025
Published online: 14 June 2025

References

1. Deedwania PC. Metabolic syndrome and vascular disease: is nature or nurture leading the new epidemic of cardiovascular disease? Circulation. 2004;109:2–4. https://doi.org/10.1161/01.CIR.0000110642.73995.BF.
2. Alberti KG, Eckel RH, Grundy SM, Zimmet PZ, Cleeman JI, Donato KA, Fruchart JC, James WPT, Loria CM, Smith SC Jr, et al. Harmonizing the metabolic syndrome: a joint interim statement of the international diabetes federation task force on epidemiology and prevention; National heart, lung, and blood institute; American heart association; world heart federation; international atherosclerosis society; and international association for the study of obesity. Circulation. 2009;120:1640–5. https://doi.org/10.1161/CIRCULATIONAHA.109.192644.
3. Ridker PM, Thuren T, Zalewski A, Libby P. Interleukin-1β Inhibition and the prevention of recurrent cardiovascular events: rationale and design of the Canakinumab Anti-inflammatory thrombosis outcomes study (CANTOS). Am Heart J. 2011;162:597–605. https://doi.org/10.1016/j.ahj.2011.06.012.
4. Ridker PM, Everett BM, Thuren T, MacFadyen JG, Chang WH, Ballantyne C, Fonseca F, Nicolau J, Koenig W, Anker SD, et al. Antiinflammatory therapy with Canakinumab for atherosclerotic disease. N Engl J Med. 2017;377:1119–31. https://doi.org/10.1056/NEJMoa1707914.
5. Libby P, Everett BM. Novel antiatherosclerotic therapies. Arterioscler Thromb Vasc Biol. 2019;39:538–45. https://doi.org/10.1161/ATVBAHA.118.310958.
6. Everett BM, MacFadyen JG, Thuren T, Libby P, Glynn RJ, Ridker PM. Inhibition of interleukin-1β and reduction in atherothrombotic cardiovascular events in the CANTOS trial. J Am Coll Cardiol. 2020;76:1660–70. https://doi.org/10.1016/j.jacc.2020.08.011.
7. Dri E, Lampas E, Lazaros G, Lazarou E, Theofilis P, Tsioufis C, Tousoulis D. Inflammatory mediators of endothelial dysfunction. Life. 2023;13:1420. https://doi.org/10.3390/life13061420.
8. Leung YY, Yao Hui LL, Kraus VB. Colchicine-Update on mechanisms of action and therapeutic uses. Sem Arthritis Rheum. 2015;45:341–50. https://doi.org/10.1016/j.semarthrit.2015.06.013.
9. Olona A, Leishman S, Anand PK. The NLRP3 inflammasome: regulation by metabolic signals. Trends Immunol. 2022;43:978–89. https://doi.org/10.1016/j.it.2022.10.003.
10. Menu P, Pellegrin M, Aubert JF, Bouzourene K, Tardivel A, Mazzolai L, Tschopp J. Atherosclerosis in ApoE-deficient mice progresses independently of the NLRP3 inflammasome. Cell Death Dis. 2011;2(3):e137. https://doi.org/10.1038/cddis.2011.18.
11. Zheng F, Xing S, Gong Z, Mu W, Xing Q. Silence of NLRP3 suppresses atherosclerosis and stabilizes plaques in Apolipoprotein E-deficient mice. Mediators Inflamm. 2014;2014:507208. https://doi.org/10.1155/2014/507208.
12. Jiang X, Wang F, Wang Y, Gisterå A, Roy J, Paulsson-Berne G, Hedin U, Lerman A, Hansson GK, Herrmann J, et al. Inflammasome-driven interleukin-1α and interleukin-1β production in atherosclerotic plaques relates to hyperlipidemia and plaque complexity. JACC Basic Transl Sci. 2019;4:304–17. https://doi.org/10.1016/j.jacbts.2019.02.007.
13. Grebe A, Hoss F, Latz E. NLRP3 inflammasome and the IL-1 pathway in atherosclerosis. Circ Res. 2018;122:1722–40. https://doi.org/10.1161/CIRCRESAHA.118.311362.
14. Martínez MC, Andriantsitohaina R. Extracellular vesicles in metabolic syndrome. Circ Res. 2017;120:1674–86. https://doi.org/10.1161/CIRCRESAHA.117.309419.
15. Malloci M, Perdomo L, Veerasamy M, Andriantsitohaina R, Simard G, Martínez MC. Extracellular vesicles: mechanisms in human health and disease. Antioxid Redox Signal. 2019;30:813–56. https://doi.org/10.1089/ars.2017.7265.
16. Agouni A, Lagrue-Lak-Hal AH, Ducluzeau PH, Mostefai HA, Draunet-Busson C, Leftheriotis G, Heymes C, Martinez MC, Andriantsitohaina R. Endothelial dysfunction caused by Circulating microparticles from patients with metabolic syndrome. Am J Pathol. 2008;173:1210–9. https://doi.org/10.2353/ajpath.2008.080228.
17. Ali S, Malloci M, Safiedeen Z, Soleti R, Vergori L, Vidal-Gómez X, Besnard C, Dubois S, Le Lay S, Boursier J, et al. LPS-enriched small extracellular vesicles from metabolic syndrome patients trigger endothelial dysfunction by activation of TLR4. Metabolism. 2021;118:154727. https://doi.org/10.1016/j.metabol.2021.154727.
18. Safiedeen Z, Rodríguez-Gómez I, Vergori L, Soleti R, Vaithilingam D, Douma I, Agouni A, Leiber D, Dubois S, Simard G, et al. Temporal cross talk between Endoplasmic reticulum and mitochondria regulates oxidative stress and mediates microparticle-induced endothelial dysfunction. Antioxid Redox Signal. 2017;26:15–27. https://doi.org/10.1089/ars.2016.6771.
19. Perdomo L, Vidal-Gómez X, Soleti R, Vergori L, Duluc L, Chwastyniak M, Bisserier M, Le Lay S, Villard A, Simard G, et al. Large extracellular vesicle-associated Rap1 accumulates in atherosclerotic plaques, correlates with vascular risks and is involved in atherosclerosis. Circ Res. 2020;127:747–60. https://doi.org/10.1161/CIRCRESAHA.120.317086.
20. Wang JG, Williams JC, Davis BK, Jacobson K, Doerschul CM, Ting JPY, Mackman N. Monocytic microparticles activate endothelial cells in an IL-1β-dependent manner. Blood. 2011;118:2366–74. https://doi.org/10.1182/blood-2011-01-330878.
21. Silvis MJM, Fiolet ATL, Opstal TSJ, Dekker M, Suquilanda D, Zivkovic M, Duyvendak M, The SHK, Timmers L, Bax WA, et al. Colchicine reduces extracellular vesicle NLRP3 inflammasome protein levels in chronic coronary disease: A LoDoCo2 biomarker substudy. Atherosclerosis. 2021;334:93–100. https://doi.org/10.1016/j.atherosclerosis.2021.08.005.
22. Zeng W, Wu D, Sun Y, et al. The selective NLRP3 inhibitor MCC950 hinders atherosclerosis development by attenuating inflammation and pyroptosis in macrophages. Sci Rep. 2021;11:19305. https://doi.org/10.1038/s41598-021-98437-3.
23. Nagar A, Rahman T, Harton JA. The ASC speck and NLRP3 inflammasome function are spatially and temporally distinct. Front Immunol. 2021;12:752482. https://doi.org/10.3389/fimmu.2021.752482.
24. Ali S, Vidal-Gomez X, Piquet M, Vergori L, Dimard G, Dubois S, Ducluzeau PH, Pomiès P, Kamli-Salino S, Delibégovic M, et al. Circulating extracellular vesicle-carried PTP1B and PP2A phosphatases as regulators of insulin resistance. Diabetologia. 2025;68:231–42. https://doi.org/10.1007/s00125-024-06288-0.
25. Duewell P, Kono H, Rayner KJ, Sirois CM, Vladimer G, Bauernfeind FG, Abela GS, Franchi L, Nuñez G, Schnurr M, et al. NLRP3 inflammasomes are required for atherogenesis and activated by cholesterol crystals. Nature. 2010;464:1357–61. https://doi.org/10.1038/nature08938.

26. Yuan X, Bhat OM, Samidurai A, Das A, Zhang Y, Li P-L. Reversal of endothelial extracellular vesicle-induced smooth muscle phenotype transition by hypercholesterolemia stimulation: role of NLRP3 inflammasome activation. Front Cell Dev Biol. 2020;8:597423. https://doi.org/10.3389/fcell.2020.597423.
27. Takahashi M. NLRP3 inflammasome as a key driver of vascular disease. Cardiovasc Res. 2022;118:372–85. https://doi.org/10.1093/cvr/cvab010.
28. Wang Z, Hu W, Lu C, Ma Z, Jiang S, Gu C, Acuña-Castroviejo D, Yang Y. Targeting NLRP3 (Nucleotide-Binding domain, Leucine-Rich-Containing family, Pyrin Domain-Containing-3) inflammasome in cardiovascular disorders. Arterioscler Thromb Vasc Biol. 2018;38:2765–79. https://doi.org/10.1161/ATVBAHA.118.311916.
29. Li H, Sun L, Wang Y. Inhibition of LPS induced NLRP3 inflammasome activation by stem cell conditioned culture media in human gingival epithelial cells. Mol Med Rep. 2023;27:106. https://doi.org/10.3892/mmr.2023.12993.
30. Park S, Shin J, Bae J, Han D, Park S-R, Shin J, Lee SK, Park H-W. SIRT1 alleviates LPS-induced IL-1β production by suppressing NLRP3 inflammasome activation and ROS production in trophoblasts. Cells. 2020;9:728. https://doi.org/10.3390/cells9030728.
31. Coll RC, Robertson AA, Chae JJ, Higgins SC, Muñoz-Planillo R, Inserra MC, Vetter I, Dungan LS, Monks BG, Stutz A, et al. A small-molecule inhibitor of the NLRP3 inflammasome for the treatment of inflammatory diseases. Nat Med. 2015;21:248–55. https://doi.org/10.1038/nm.3806.
32. Pavillard LE, Cañadas-Lozano D, Alcocer-Gómez E, Marín-Aguilar F, Pereira S, Robertson AAB, Muntané J, Ryffel B, Cooper MA, Quiles JL, et al. NLRP3-inflammasome Inhibition prevents high fat and high sugar diets-induced heart damage through autophagy induction. Oncotarget. 2017;8:99740–56. https://doi.org/10.18632/oncotarget.20763.
33. DeSena AD, Do T, Schulert GS. Systemic autoinflammation with intractable epilepsy managed with interleukin-1 Blockade. J Neuroinflammation. 2018;15:38. https://doi.org/10.1186/s12974-018-1063-2.
34. Welsh JA, Goberdhan DCI, O'Driscoll L et al. Minimal information for studies of extracellular vesicles (MISEV2023): From basic to advanced approaches [published correction appears in J Extracell Vesicles. 2024;13(5):e12451. doi: 10.1002/jev2.12451]. J Extracell Vesicles. 2024;13(2):e12404. https://doi.org/10.1002/jev2.12404
35. Lafuente N, Matesanz N, Azcutia V, et al. The deleterious effect of high concentrations of D-glucose requires pro-inflammatory preconditioning. J Hypertens. 2008;26:478–85. https://doi.org/10.1097/hjh.0b013e3282f331fb
36. Peiró C, Romacho T, Azcutia V, et al. Inflammation, glucose, and vascular cell damage: the role of the Pentose phosphate pathway. Cardiovasc Diabetol. 2016;15:82. https://doi.org/10.1186/s12933-016-0397-2
37. Leroyer AS, Isobe H, Lesèche G, et al. Cellular origins and thrombogenic activity of microparticles isolated from human atherosclerotic plaques. J Am Coll Cardiol. 2007;49:772–7. https://doi.org/10.1016/j.jacc.2006.10.053

Publisher's note